General Disclaimer

- This document has been reproduced from the best copy furnished by the organizational source. It is being released in the interest of making available as much information as possible.

- This document may contain data, which exceeds the sheet parameters. It was furnished in this condition by the organizational source and is the best copy available.

- This document may contain tone-on-tone or color graphs, charts and/or pictures, which have been reproduced in black and white.

- This document is paginated as submitted by the original source.

- Portions of this document are not fully legible due to the historical nature of some of the material. However, it is the best reproduction available from the original submission.

LEHIGH UNIVERSITY

INSTITUTE OF RESEARCH

CYLINDRICAL AND SPHERICAL SHELLS WITH CRACKS

by
F. Erdogan
J. Kibler

October 1968

CYLINDRICAL AND SPHERICAL SHELLS WITH CRACKS

by

F. Erdogan and J. Kibler

Prepared under Grant No. NGR 39-007-011 by

LEHIGH UNIVERSITY

Bethlehem, Pennsylvania

for

NATIONAL AERONAUTICS AND SPACE ADMINISTRATION

October 1968

CYLINDRICAL AND SPHERICAL SHELLS WITH CRACKS

by

F. Erdogan and J. Kibler

SUMMARY

The symmetric problem for the cylindrical and spherical shells containing a meridional crack is considered. The problem is solved for a uniform membrane load and a uniform bending moment applied to the surface of the crack. The extensional and bending components of the stress intensity factor ratio are obtained as functions of shell parameter and are tabulated. The results are also plotted in order to compare them with the existing asymptotic solutions.

INTRODUCTION

A meridional crack in cylindrical and spherical shells subjected to internal pressure was considered by Folias [1,2]. After obtaining the respective systems of integral equations for the cylinder and the sphere, Folias gave asymptotic expressions for the stress intensity factors for both cases. These expressions are valid only for small values of shell parameter λ, hence their range of application is limited. In this paper, the integral equations are solved numerically and the stress intensity factors are evaluated for up to $\lambda = 8$ in cylindrical shells and up to $\lambda = 5$ in spherical shells.

THE SOLUTION AND RESULTS

To analyze the stress singularities at the ends of meridional cracks in isotropic and homogeneous thin shells, in [1] and [2], the following linearized shallow-shell equations were used, which are due to Marguerre [3] and Reissner [4] :

$$\frac{Eha^2}{R}\frac{\partial^2 W}{\partial x^2} + \nabla^4 F = 0$$

$$\nabla^4 W - \frac{a^2}{RD}\frac{\partial^2 F}{\partial x^2} = \frac{q}{D}a^4 \qquad (1)$$

for cylindrical shells, and

$$-\frac{Eha^2}{R}\nabla^2 W + \nabla^4 F = 0$$

$$\nabla^4 W + \frac{a^2}{RD}\nabla^2 F = \frac{q}{D}a^4 \qquad (2)$$

for spherical shells. In (1) and (2), X, Y, Z are the rectangular coordinates with Z normal to the surface and X in the plane of the crack, W is the displacement in Z direction, $x = X/a$, $y = Y/a$ are dimensionless coordinates, a is the half-crack length, R is the mean radius, h is the shell thickness, F is the stress function, q is the normal traction acting on the shell surface, E is the Young's modulus and D is the flexural rigidity, $D = Eh^3/12(1-\nu^2)$, ν being the Poisson's ratio. In the usual manner, the components of bending moment M_x, M_y, M_{xy} and transverse shear Q_x, Q_y are given in terms of W and

the membrane forces N_x, N_y, N_{xy} are given in terms of F.

In general, the singular solution of the cracked shell problem may be reduced to a perturbation problem in which self-equilibrating forces and moments acting on the crack surfaces are the only external loads. Thus, in one class of important symmetric problems, the homogeneous systems obtained from (1) and (2) will have to be solved with the following boundary conditions on the crack surface

$$M_y = M_o(x),\ V_y = Q_y + \frac{\partial M_{xy}}{\partial x} = 0, \tag{3}$$

$$N_y = N_o(x),\ N_{xy} = 0,\ (-1<x<1,\ y = 0)$$

and vanishing stresses away from the crack. Due to the conditions of symmetry, in [1] and [2], the functions F(x,y) and W(x,y) are expressed in terms of Fourier cosine integrals, and the resulting dual integral equations are reduced to a system of singular integral equations of the following form*

$$\int_{-1}^{1} \sum_{1}^{2} h_{ij}(x,t)u_j(t)dt = f_i(x),\ (i = 1,2;\ -1<x<1) \tag{4}$$

where the kernels h_{ij} contain Cauchy-type singularities, u_1,

*For details of the analysis and explicit forms of the kernels h_{ij}, see [5] and [6].

u_2 are conveniently defined unknown functions *and* f_1, f_2 are related to the external loads. For example, for constant M_y and N_y in (3), letting

$$M_o = \frac{m_o D}{a^2}, \quad N_o = \frac{n_o}{a^2} \tag{5}$$

we have

$$f_1(x) = \frac{2\pi n_o}{i\sqrt{EDh}}\, x, \quad f_2(x) = -\, 2\pi m_o x \tag{6}$$

The kernels $h_{ij}(x,t)$ in (4) contain modified Bessel functions of the form, $K_j(e^{\mp \pi i/4}|t-x|\lambda/n)$, $(j = 0,1)$, where $n = 2$ for cylindrical shells, $n = 1$ for spherical shells and λ is the shell parameter defined by

$$\lambda = [12(1-\nu^2)]^{1/4} \frac{a}{\sqrt{Rh}}$$

Here ν is the Poisson's ratio, a is the half crack length, R is shell radius of curvature and h is the shell thickness.

Studying the asymptotic values of the kernels for small arguments, it is easily shown that at $t = x$, h_{ij} are singular and the leading terms are of the form $a_{ij}/(t-x)$, where a_{ij}, $(i,j = 1,2)$, are constant. For convenience in the numerical analysis, we replace the modified Bessel functions having complex arguments by the Kelvin functions with real arguments by using the following relation:

$$e^{-\frac{1}{2}\nu\pi i} K_\nu(xe^{\pi i/4}) = ker_\nu x + ikei_\nu x \tag{7}$$

Around zero, the functions ker_1 and kei_1 behave like $1/x$ which provide the singularity of the integral equations and may easily be separated. By using the polynomial approximations for the functions ker_ν and kei_ν, ($\nu = 1,2$) given in [7], (4) may be put in the following form:

$$\int_{-1}^{1} \sum_{1}^{2} a_{ij} u_j(t) \frac{dt}{t-x} + \int_{-1}^{1} k_{ij}(x,t) u_j(t) dt = f_i(x) \tag{8}$$

$$i = 1,2, \quad |x|<1$$

where the coefficients a_{ij} are known constants and the kernels k_{ij} are bounded known functions.

From the definitions of the auxiliary functions u_1 and u_2 as given in [1] and [2], it can be shown that u_1 and u_2 are even functions and the index of the system of equations (8) is -1, that is u_1 and u_2 may be expressed as

$$u_j(x) = \sqrt{1-x^2}\, A_j(x^2), \quad (j = 1,2) \tag{9}$$

where the functions A_1, A_2 are regular. Again, referring to [1] and [2] for details, we simply note that the extensional and bending components of the stress intensity factors are directly related to the values of the functions A_j at $x = 1$. Hence the solution of (8) is sufficient for the evaluation of

stress intensity factors.

The system of singular integral equations (8) may be regularized by using the method of Muskhelishvili [8] or Carlemann and Vekua [9]. However, because of the complexity of the kernels k_{ij}, the process is quite complicated and the solution of the resulting system of integral equations with weakly singular kernels can only be solved approximately. Therefore, to solve (8), we use the method described in [10], which is based on the observation that the fundamental function of the system (8) is the weight of Chebishev polynomials. Thus, the singularities of (8) may be removed by expressing the functions A_j as infinite series in these orthogonal polynomials. The technique is rather easy to apply and allows introducing into the program an automatic convergence scheme for a desired degree of accuracy in the computed quantities (by simply specifying the number of significant digits in stress intensity ratios which should be repeated as the number of terms in the series is increased).

Here, we give the numerical results for four different cases, namely the cylindrical and the spherical shells with the loading conditions $N_o \neq 0$, $M_o = 0$ and $N_o = 0$, $M_o \neq 0$. Let the stress intensity factors in shells be

$$k_s = (A_e + A_b)k_p \text{ (outer surface)}$$
$$k_s = (A_e - A_b)k_p \text{ (inner surface)} \qquad (10)$$

where k_p is the stress intensity factor in the corresponding flat plate and is given by

$$k_p = \frac{N_o}{h}\sqrt{a}, \text{ for } N_o \neq 0,\ M_o = 0$$
$$k_p = \frac{6M_o}{h^2}\sqrt{a}, \text{ for } M_o \neq 0,\ N_o = 0 \qquad (11)$$

The constants A_e and A_b are the extensional and bending components of the stress intensity factor and are given in Tables 1 and 2, either directly (A_e for $N_o \neq 0$, $M_o = 0$ and A_b for $N_o = 0$, $M_o \neq 0$) or through the following relations

$$A_b = \frac{(3+\nu)}{\sqrt{(1-\nu^2)/3}}\, a_b \text{ for } N_o \neq 0,\ M_o = 0$$
$$(12)$$
$$A_e = \sqrt{(1-\nu^2)/3}\, a_e \text{ for } N_o = 0,\ M_o \neq 0$$

Regarding the results given by Tables 1 and 2, the following should be noted: a) the Poisson's ratio ν appears explicitly as well as through λ in the expressions for k_{ij}. Thus the numerical results are obtained for one value of ν only, which was selected to be $\nu = 1/3$. b) Because of the assumption of Kirchhoff type boundary conditions in the formulation of the problem, the angular distributions of extensional and bending stresses around the crack tip are not the same, hence the superposition given by (10) is valid only for $\theta = 0$, that is, along the prolongation of the crack. c) The numerical

analysis is carried out by using polynomial approximations for Kelvin functions which are valid in $-8 \leq x \leq 8$ with a residual error of less than 10^{-7}, x being the argument of the functions. In the cylindrical shells, the argument x varies in $0 \leq x \leq \lambda$, and in spherical shells, in $0 \leq x \leq \lambda/2$. Since we required only four significant digit accuracy in the calculated quantities, technically, we could obtain useful results for values of λ somewhat larger than 8 in cylinders and 4 in spheres. To obtain more reliable results for higher values of λ, in addition to polynomial approximations valid for small x, one can also introduce the asymptotic expressions for the Kelvin functions valid for $|x|>8$ (also given in [7]).

The results given in Tables 1 and 2 are shown in Figures 1-8. The figures also include the results of the asymptotic solutions obtained in [1] and [2].

Comparison of the two sets of curves clearly indicates the inadequacy of the asymptotic solutions for moderately large values of λ. Note that at $\lambda = 0$, as expected, all stress intensity ratio curves have zero slope. Note also that the effect of shell curvature on the stress intensity factors is much more significant if the shell is subjected to membrane loading rather than bending.

REFERENCES

1. Folias, E. S., Int. J. Fracture Mechanics, 1, 1965, 104.

2. Folias, E. S., Int. J. Fracture Mechanics, 1, 1965, 20.

3. Marguerre, K., Proc. 5th Int. Congress Appl. Mech. 1938, 93.

4. Reissner, E. in "Structural Mechanics", Proc. 1st Symposium on Naval Structural Mechanics, Pergamon, 1960, 74.

5. Folias, E. S., ARL 64-174, Aerospace Research Laboratories, Office of Aerospace Research, U.S. Air Force, October 1964.

6. Folias, E. S., ARL 64-23, Aerospace Research Laboratories, Office of Aerospace Research, U.S. Air Force, January 1964.

7. Abramowitz, M. and Stegun, I. A., Editors, "Handbook of Mathematical Functions", National Bureau of Standards, Appl. Math. Series 55, 1964.

8. Muskhelishvili, N. I., "Singular Integral Equations", P. Noordhoff N. V., Groningen Holland, 1953.

9. Pogorzelshi, W., "Integral Equations and Their Applications", Vol. 1, Pergamon, 1966.

10. Erdogan, F., to appear in SIAM Journal on Applied Mathematics, 1969.

Table 1 - Stress Intensity Factor Ratios For

$N_o \neq 0$, $M_o = 0$

	CYLINDER		SPHERE	
λ	A_e	a_b	A_e	a_b
.2	1.0096	.00410	1.0112	.00611
.4	1.0371	.01124	1.0422	.01693
.6	1.0795	.01902	1.0887	.02919
.8	1.1344	.02659	1.1479	.04186
1.0	1.1993	.03359	1.2174	.05448
1.2	1.2723	.03985	1.2956	.06685
1.4	1.3519	.04529	1.3812	.07886
1.6	1.4367	.04990	1.4731	.09045
1.8	1.5256	.05368	1.5706	.10155
2.0	1.6177	.05664	1.6729	.11216
2.2	1.7122	.05883	1.7795	.12223
2.4	1.8085	.06018	1.8899	.13172
2.6	1.9060	.06090	2.0038	.14058
2.8	2.0045	.06083	2.1208	.14879
3.0	2.1035	.06014	2.2408	.15630
3.25	2.2276	.05832	2.3947	.16463
3.50	2.3519	.05549	2.5526	.17172
3.75	2.4761	.05172	2.7143	.17751
4.00	2.5999	.04700	2.8796	.18194
4.25	2.7232	.04154	3.0485	.18483
4.50	2.8459	.03512	3.2208	.18644
5.00	3.0895	.02012	3.5750	.18493
5.50	3.3303	.00234	3.9446	.17802
6.00	3.5681	-.02222		
6.50	3.8029	-.04130		
7.00	4.0347	-.06622		
7.50	4.2637	-.09350		
8.00	4.4895	-.12279		

Table 2 - Stress Intensity Factor Ratios For

$N_o = 0, M_o \neq 0$

	CYLINDER		SPHERE	
λ	a_e	A_b	a_e	A_b
.2	.006161	.99816	.00842	1.0020
.4	.01695	.99340	.02249	1.0070
.6	.02897	.98660	.03749	1.0137
.8	.04107	.97846	.05202	1.0211
1.0	.05283	.96946	.06557	1.0287
1.2	.06406	.95986	.07799	1.0364
1.4	.07473	.94993	.08935	1.0439
1.6	.08482	.93976	.09964	1.0512
1.8	.09435	.92956	.10895	1.0583
2.0	.1033	.91936	.11740	1.0652
2.2	.1118	.90923	.12519	1.0718
2.4	.1198	.89926	.13228	1.0783
2.6	.1273	.88940	.13876	1.0845
2.8	.1344	.87970	.14475	1.0905
3.0	.1410	.87023	.15030	1.0964
3.25	.1488	.85863	.15668	1.1035
3.50	.1551	.84740	.16260	1.1103
3.75	.1628	.83643	.1681	1.1170
4.00	.1691	.82440	.1732	1.1233
4.25	.1750	.81542	.1780	1.1297
4.50	.1803	.80539	.1826	1.1357
5.00	.1903	.78616	.1905	1.1470
5.50	.2005	.76832	.2000	1.1580
6.00	.2068	.75079		
6.50	.2137	.73446		
7.00	.2200	.71879		
7.50	.2255	.7080		
8.00	.2306	.6897		

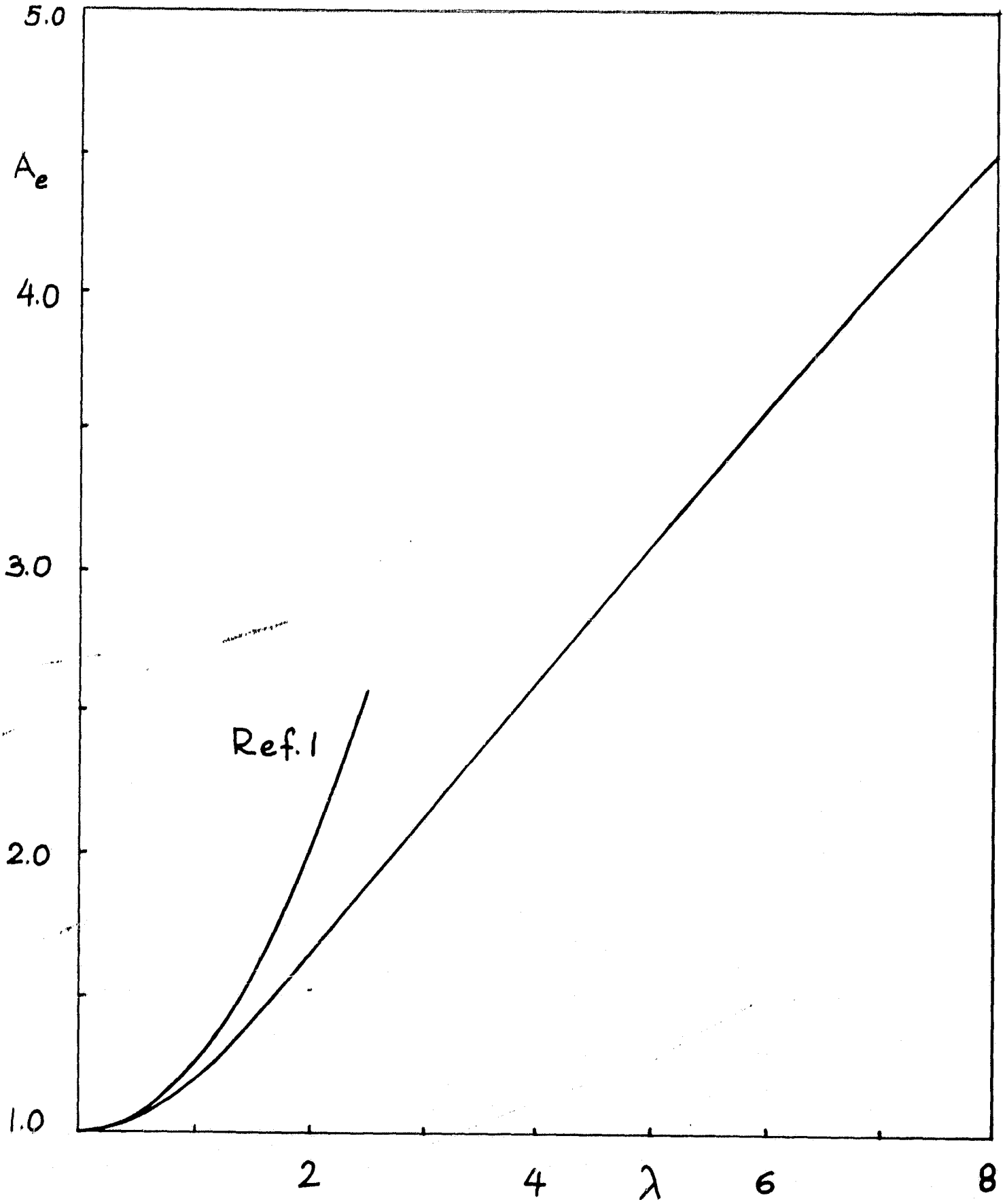

Figure 1. Stress intensity ratio in cylinder ($N_o \neq 0, M_o = 0$)

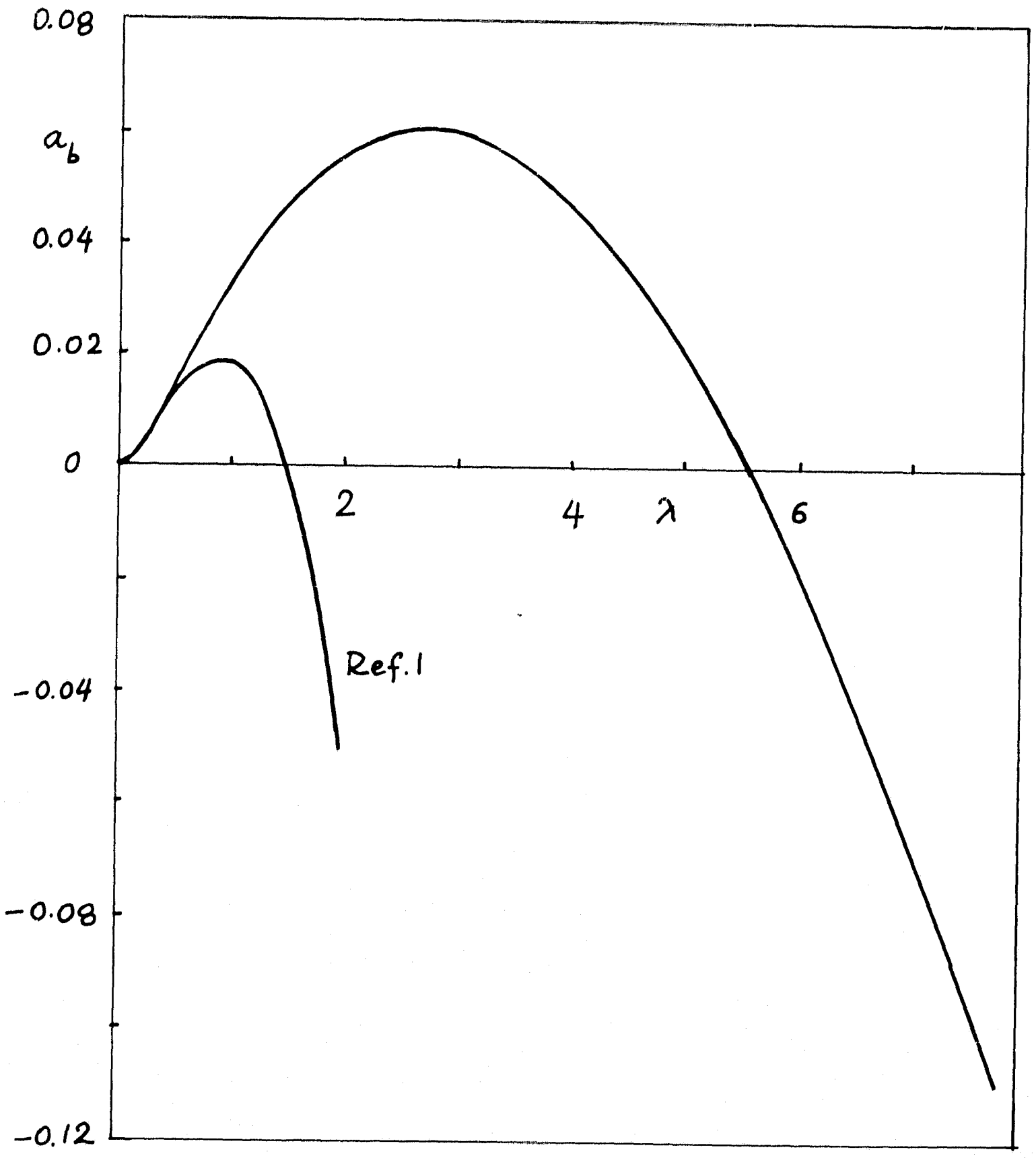

Figure 2. Stress intensity ratio in cylinder ($N_o \neq 0, M_o = 0$)

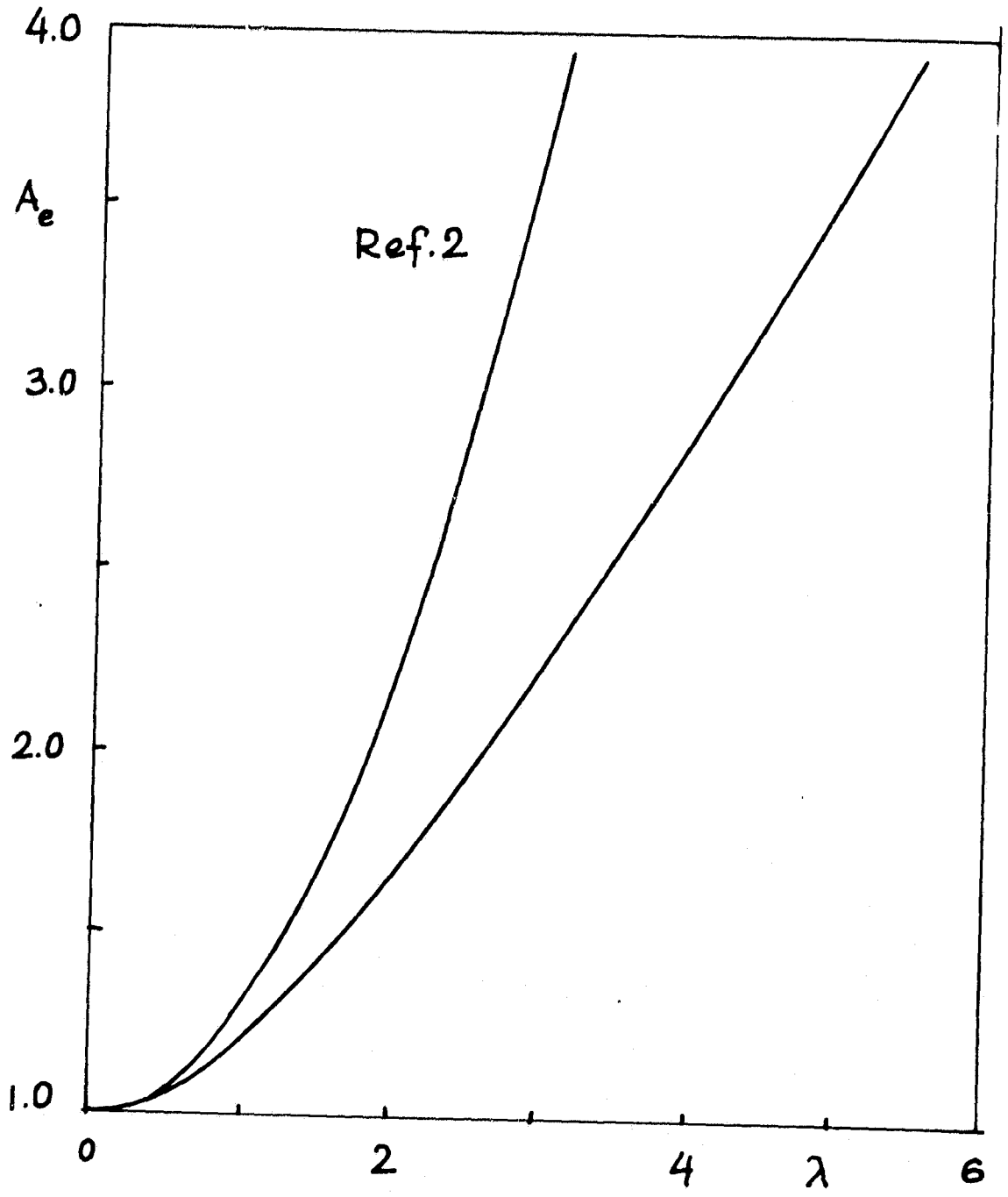

Figure 3. Stress intensity ratio in sphere ($N_o \neq 0, M_o = 0$)

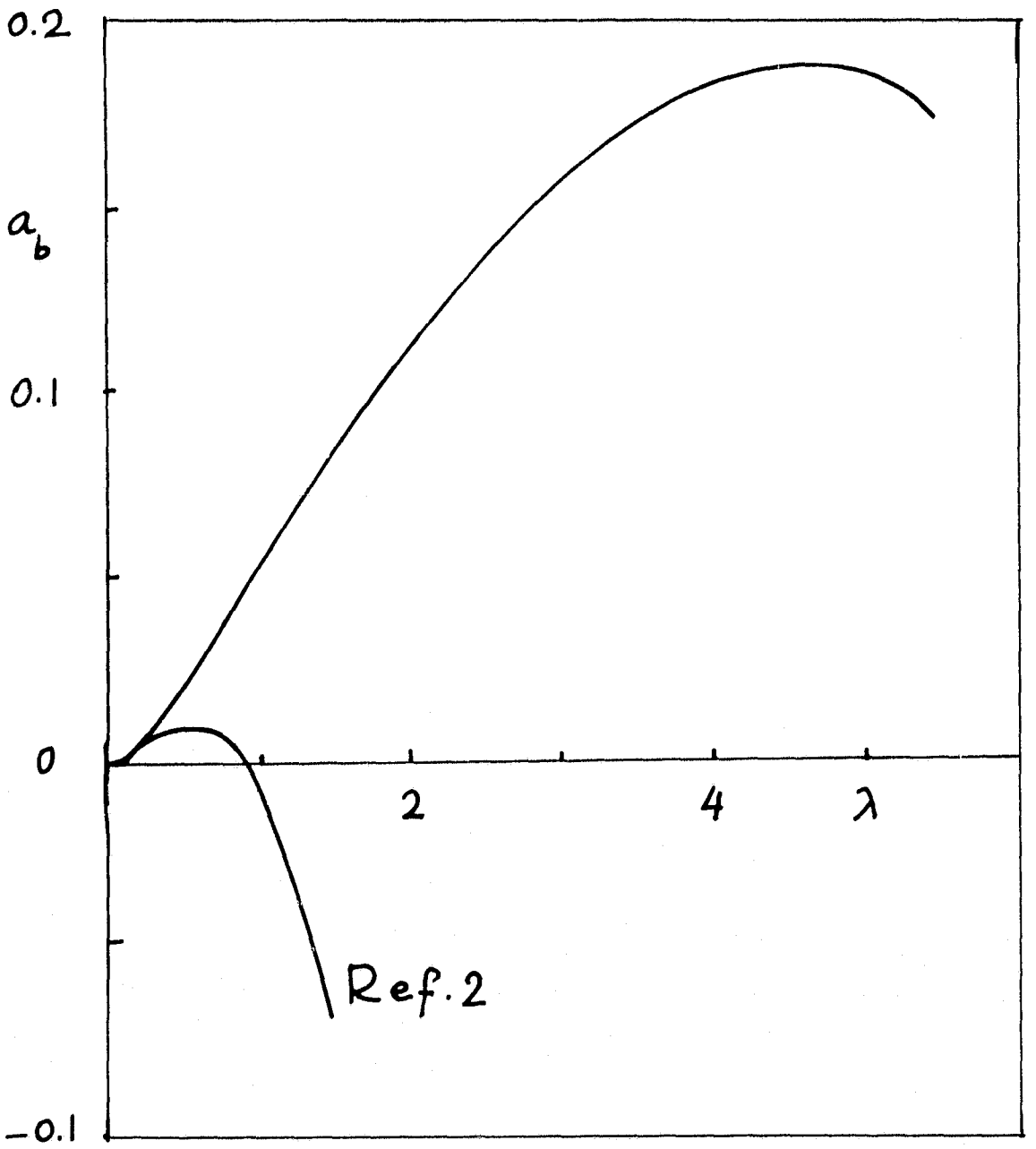

Figure 4. Stress intensity ratio in sphere ($N_o \neq 0, T_o = 0$)

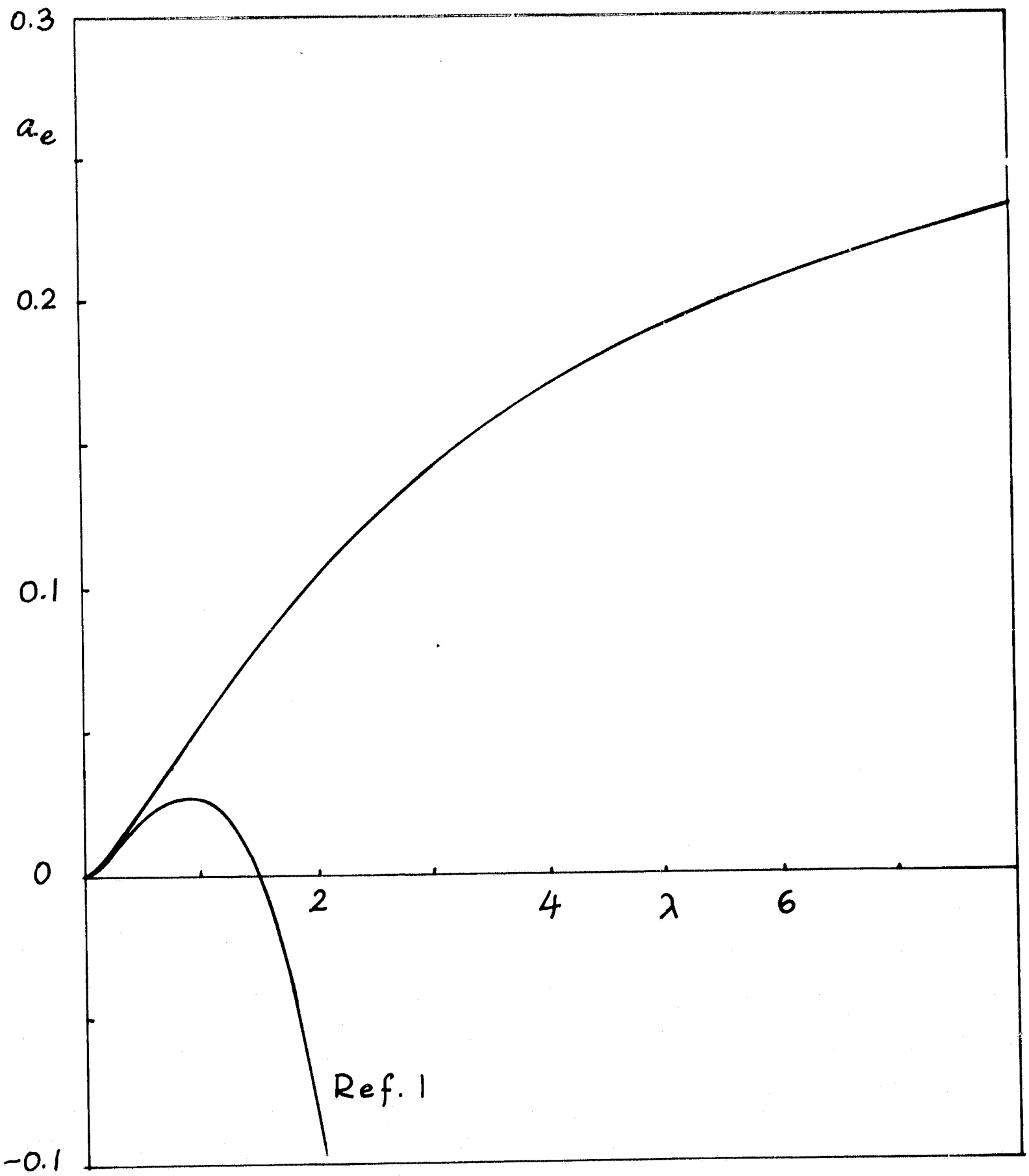

Figure 5. Stress intensity ratio in cylinder ($N_o=0, M_o\neq 0$)

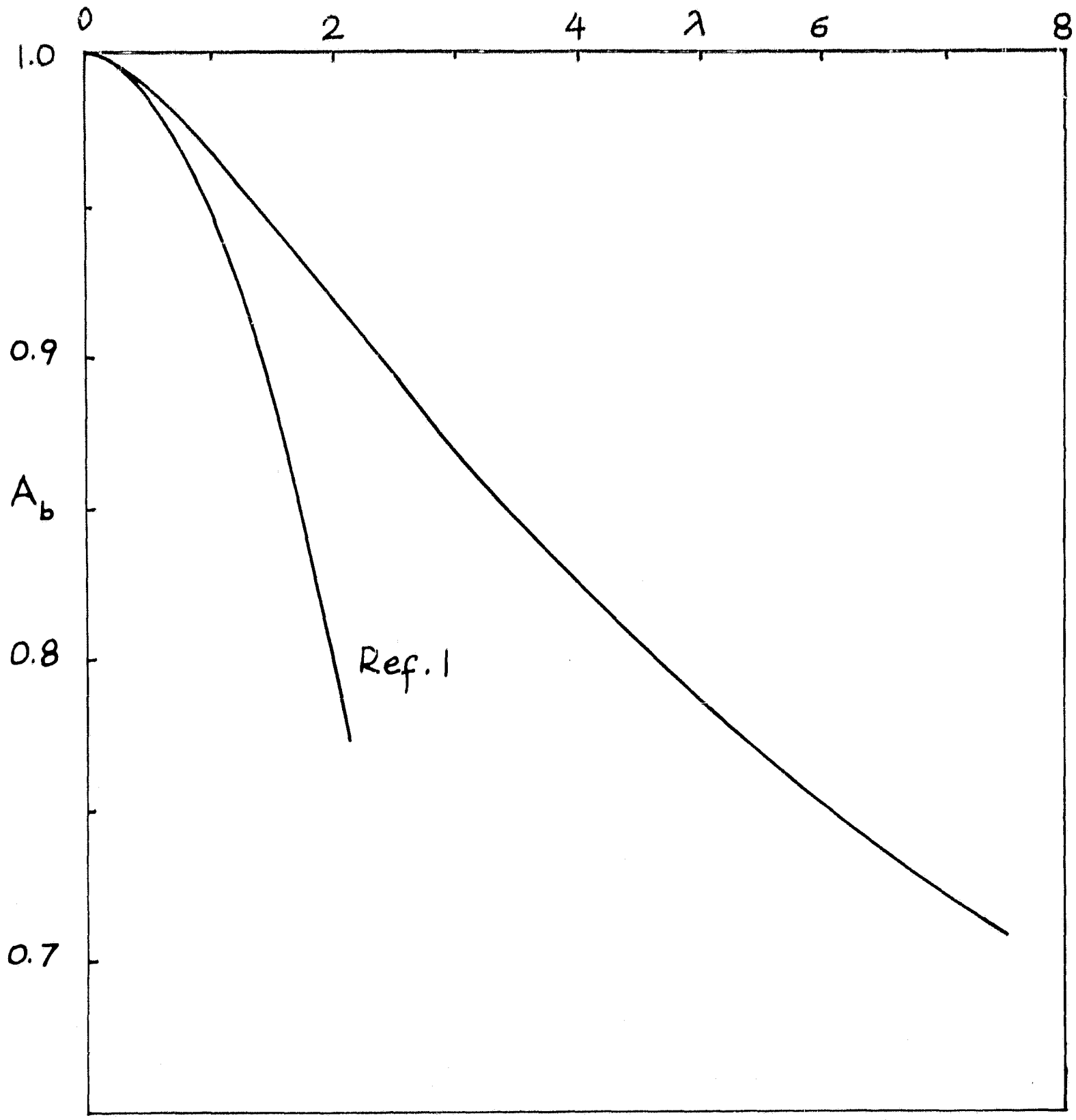

Figure 6. Stress intensity ratio in cylinder ($H_0=0, H_0\neq 0$)

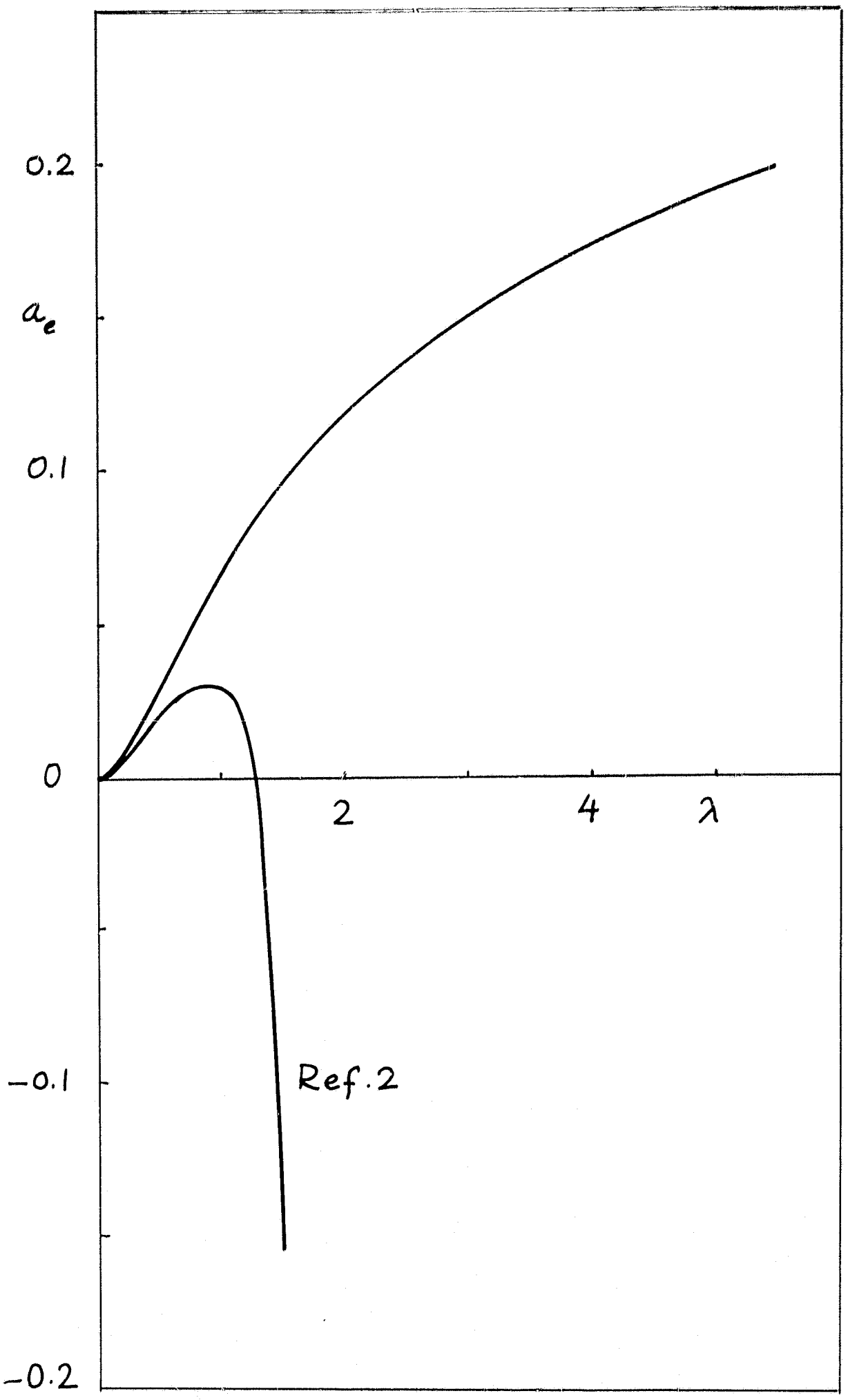

Figure 7. Stress intensity ratio in sphere ($N_o=0, M_o\neq 0$)

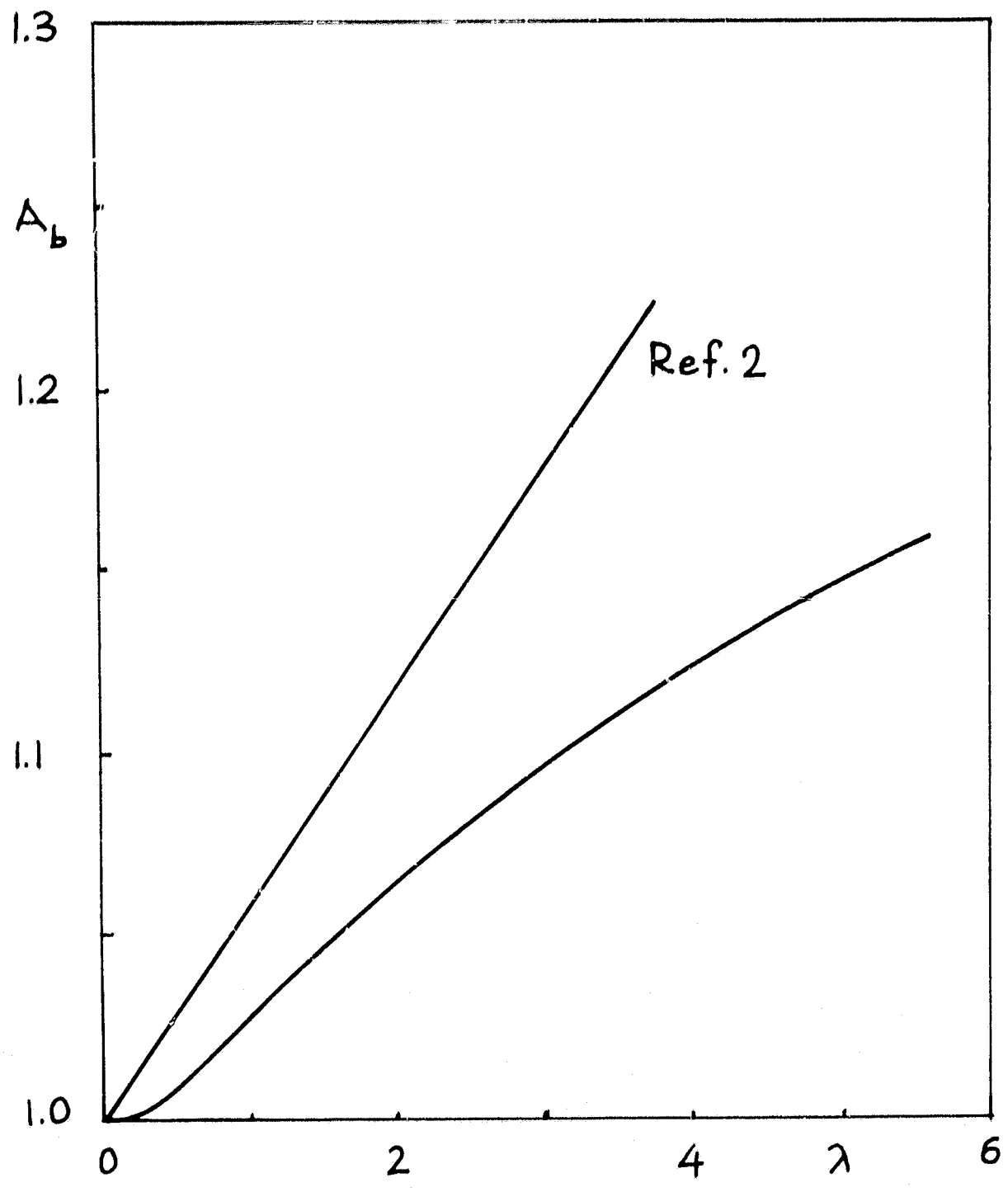

Figure 8. Stress intensity ratio in sphere ($H_o=0, H_o\neq 0$)